Novel Acyclic Deoxystreptamine Mimetics Targeting the Ribosomal Decoding Site

Dionisios Vourloumis,*[a] Geoffrey C. Winters,[a] Masayuki Takahashi,[a] Klaus B. Simonsen,[a] Benjamin K. Ayida,[a] Sarah Shandrick,[b] Qiang Zhao,[b] and Thomas Hermann*[b]

KEYWORDS:

aminoglycosides · antibiotics · drug design · medicinal chemistry · RNA recognition

Natural aminoglycoside antibiotics such as paromomycin and neomycin B[1] disrupt functional protein synthesis in bacteria by specifically binding to the decoding-site RNA in the 30S ribosomal subunit (Figure 1),[2] thereby interfering with mRNA decoding fidelity and ultimately leading to bacterial cell death. Binding of the aminoglycosides to the decoding site displaces two adenine residues (A1492 and A1493) from the deep groove of the internal-loop RNA. This displacement facilitates the utilization of noncognate tRNAs and leads to decreased translational accuracy.[3, 4] While the efficacy of natural aminoglycosides as antibiotics is compromised by bacterial resistance and undesirable pharmacological profiles,[5] their capability to bind with high affinity to the bacterial decoding site and other distinct RNA targets,[6] such as ribozymes and viral regulatory domains, renders them a lead paradigm in RNA molecular recognition.[7–9] Aminoglycosides thus provide starting points for the design of novel RNA binders.[9–15] The daunting challenge of selective derivatization of the highly functionalized natural products has encouraged efforts to discover novel antibacterial ligands directed at the decoding site by starting from smaller fragments of aminoglycosides (Figure 1). Previous approaches to the synthesis of simplified aminoglycosides have focused on derivatization of 2-deoxystreptamine (2-DOS), as an individual moiety[10, 11] or in the context of the neamine[12] and paromamine[13, 14] scaffolds, and on derivatization of the glucosamine fragment.[15] The availability of three-dimensional structures for aminoglycoside complexes of the bacterial decoding-site RNA[16, 17] and whole 30S ribosomal subunits[4, 18] has prepared the ground for rational structure-based design of readily accessible aminoglycoside mimetics. These will provide lead compounds for the development of novel antibiotics that achieve RNA target binding affinity, specificity, and antibacterial potency comparable to those of the natural products, and whose efficacy may not be compromised by bacterial resistance mechanisms specific to the natural products.

Herein and in the accompanying report,[19] we outline novel strategies for linking the 6′-aminoglucosamine moiety, conserved among many potent natural aminoglycosides, to alternative scaffolds that mimic the unique spatial arrangement of the functional groups in 2-DOS that are required for the recognition of the RNA target. The novel scaffolds were designed by molecular modeling[20] based on the crystal structure of paromomycin complexed with the bacterial decoding site (Figure 1).[4, 16–18] In this report, we describe the synthesis and testing of 37 6′-aminoglucosamine derivatives comprising two different series of acyclic 2-DOS mimetics (**1** and **2**, Figure 1 c – e). Series **1** was conceived to emulate the interactions of the 2-DOS amino group at the 1-position while providing additional interactions with the decoding-site RNA through substituents R^2 and R^3 (Figure 1 c). Series **2** was designed to make contacts to the RNA similar to those made by the groups at the 4- and 5-positions of 2-DOS, with emphasis on nonsaccharide moieties R^1, which replaces the furanose-pyranose fragment at the 5-position in paromomycin and neomycin (Figure 1 c). The amino group at the 4-position, present in all compounds of Series **2**, may exploit a potential interaction with the tightly bound water molecule at the deep-groove edge of the U1406◦U1495 base pair in the bacterial decoding-site RNA (Figure 1 e).

Our synthetic efforts commenced from 2-acetamido-2-deoxy-D-glucopyranose (**3**), which was treated with acetic anhydride and triethylamine in the presence of a catalytic amount of 4-DMAP to yield the peracetylated product quantitatively (Scheme 1). Subsequent treatment with phenylthiotrimethylsilane in the presence of zinc iodide[21] produced the corresponding glycosyl donor in 89% yield. The free amine was obtained by basic hydrolysis of the acetates and transformed into the corresponding azide **4** by reaction with triflic azide (TfN_3) in 80% overall yield.[22] Selective tosylation of the primary hydroxy group was accomplished by treatment with stoichiometric amounts of tosyl chloride in pyridine. Treatment of the corresponding tosylate with sodium azide resulted in the formation of diazido compound **5** in 97% yield. Step-economy considerations suggested the use of 2-(azidomethyl)benzoyl for the protection of the resulting diol.[23, 24] Thus, AZMB-Cl was synthesized from methyl 2-methylbenzoate (**6**) through a previously described 3-step sequence[23, 24] and treated with diol **5** in the presence of 4-DMAP to produce diester **8** in 88% yield.

To obtain compounds following the general design of Series **1** (Figure 1 c), a variety of commercially available 1,2-hydroxylamines (**a** – **c**, **g** – **k**, **o**, Scheme 1) were coupled with the glycosyl donor, after *N*-protection through the corresponding azides, by previously described methods (Scheme 1).[22] To access representatives of the designed Series **2** (Figure 1 c), some genuine 1,2- and 1,3-hydroxy amines (**d** – **f**, **l** – **n**, Scheme 1) were considered as well, all of which were easily accessible through short synthetic sequences (Scheme 2). Coupling of bis-AZMB-glycosyl

[a] *Dr. D. Vourloumis, G. C. Winters, M. Takahashi, Dr. K. B. Simonsen, Dr. B. K. Ayida*
Department of Medicinal Chemistry
Anadys Pharmaceuticals, Inc.
9050 Camino Santa Fe, San Diego, CA 92121 (USA)
E-mail: dvourloumis@anadyspharma.com

[b] *Dr. T. Hermann, S. Shandrick, Dr. Q. Zhao*
Departments of RNA Biochemistry and Structural Chemistry
Anadys Pharmaceuticals, Inc.
9050 Camino Santa Fe, San Diego, CA 92121 (USA)
Fax: (+1) 858-527-1539
E-mail: thermann@anadyspharma.com

 DOI: 10.1002/cbic.200300688 © 2003 Wiley-VCH Verlag GmbH & Co. KGaA, Weinheim

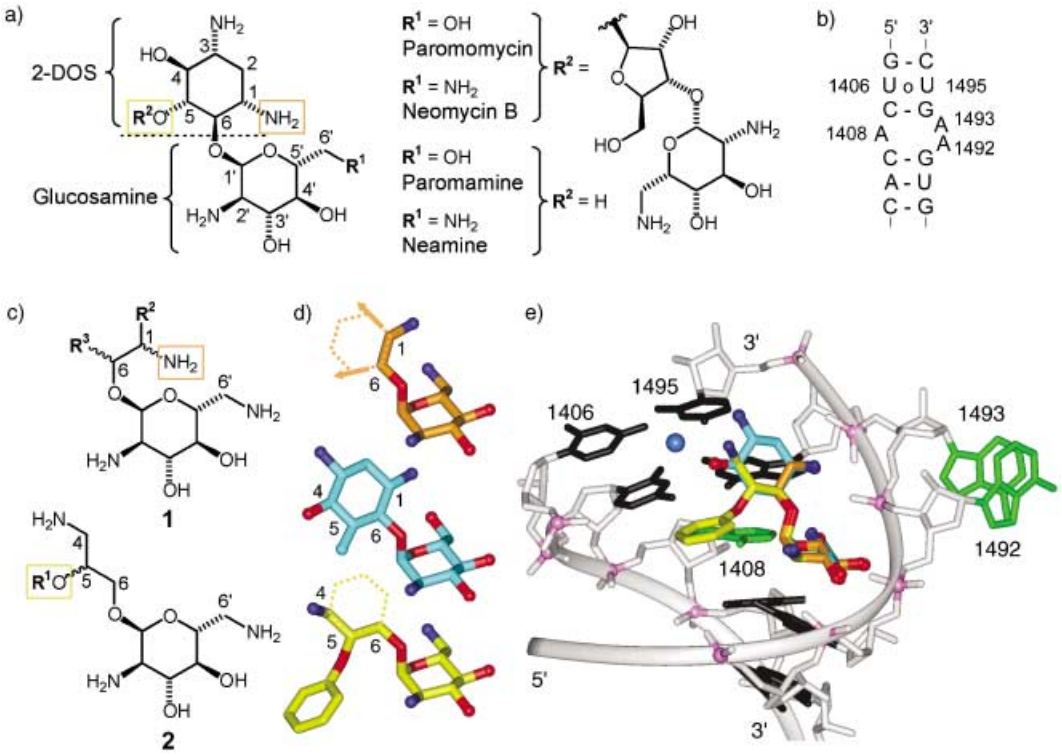

*Figure 1. a) Potent natural aminoglycoside antibiotics such as paromomycin and neomycin B are derived from paromamine and neamine, which share the 2-deoxystreptamine (2-DOS) and glucosamine cores, both of which are involved in RNA molecular recognition. b) Secondary structure of the bacterial decoding-site RNA. c) Design concept of ligands **1** and **2** for the decoding-site RNA, derived by coupling 6′-aminoglucosamine with acyclic moieties acting as 2-DOS mimetics. Corresponding positions in the designed ligands and 2-DOS are boxed and numbered accordingly. d) Three-dimensional models of the designed ligands (**1**, orange and **2**, yellow) showing their conformational similarity with paromamine (blue, center). Vectors of substituents R^2 and R^3 in ligand series **1** are indicated by arrows. The approximate position of the corresponding cyclohexane backbone in 2-DOS is indicated by dashed lines. Note that the vector of the R^1 substituent in **2** coincides with that of the 5-position of paromamine, where the furanose substituent is linked in paromomycin. e) Models of the designed ligands (**1**, orange and **2**, yellow) docked in the three-dimensional structure[18] of the bacterial decoding-site RNA in complex with paromomycin (blue; only paromamine core shown). RNA bases are in dark grey, and the sugar – phosphate backbone is in light grey with phosphate groups emphasized in magenta. A water molecule participating in the non-Watson – Crick U1406◦U1495 base pair[16] and interacting with a 2-DOS hydroxy group is shown as a blue sphere. The flipped-out adenine residues 1492 and 1493, and the unpaired adenine 1408 are shown in green.*

donor **8** with alcohols XH (Scheme 1) by standard methods (NIS, TfOH) resulted in the formation of protected aminoglycoside mimetics **9a**–**o** in good yields (61–88%). Deprotection of the individual silyl- and PMB-ethers in **9l** and **9e**, respectively, followed by a global Staudinger reduction of the azide functionalities and concurrent AZMB cleavage through a cyclo-release mechanism,[23] gave the aminoglycoside mimetics **10a**–**k**, **10m**–**o** in 50–92% yields after chromatography.

The intriguing difference between the potencies of benzylic ether **16a** and alcohol **10m** as inhibitors of bacterial in vitro translation (Table 1) directed our efforts to analogues bearing a benzylic-type functionality attached through an ether linkage on the newly introduced hydroxy group. The synthesis of the desired building blocks **12** and **13** was initiated from *R*-(+)-glycidol (**11**), which was initially treated with *p*-methoxybenzyl chloride and NaH in DMF to yield the corresponding PMB-ether (Scheme 2). The epoxide functionality was regioselectively opened by treatment with sodium azide in the presence of ammonium chloride to furnish alcohol **12** in 93% yield for the two steps. Protection of the secondary hydroxy group in **12** as the corresponding silylether (TBS-OTf, 2,6-lutidine), followed by oxidative cleavage of the PMB-ether induced by CAN, produced primary alcohol **13** in 93% overall yield. Coupling of bis-PMB-ether **14** (obtained by treating diol **5** with PMB-Cl and NaH (85% yield)) and alcohol **13** under the previously described glycosylation conditions (Scheme 1), followed by TBAF-induced cleavage of the silyl ether, furnished glycoside **15** as the pure α-anomer in 66% overall yield. A variety of commercially available benzylic halides were coupled to alcohol **15** under basic conditions, which produced the desired ethers in very good yields (Scheme 2). Oxidative cleavage of the PMB-ethers followed by Staudinger reduction yielded aminoglycoside mimetics **16a**–**p** in excellent overall yields. A similar sequence with *S*-(−)-glycidol (**17**) as the chiral starting material led to the glycoside isomers **20a**, **20b**, **20f**, and **20o**, used for direct comparison (Scheme 2) with **16**. Displacement of the hydroxy group in **19** with an azide through a two-step sequence (MsCl in pyridine followed by NaN_3 in DMF) produced tetraamine **22** after the final deprotections. In a variant approach, allyl ether **23** was ozonolyzed to produce the corresponding aldehyde, which was used in a series of reductive aminations, as presented in Scheme 3. The products **24a**–**c** were finally deprotected as described above, which resulted in aminoglycoside mimetics **25a**–**c** in 8-19% overall yields.

 © 2003 Wiley-VCH Verlag GmbH & Co. KGaA, Weinheim

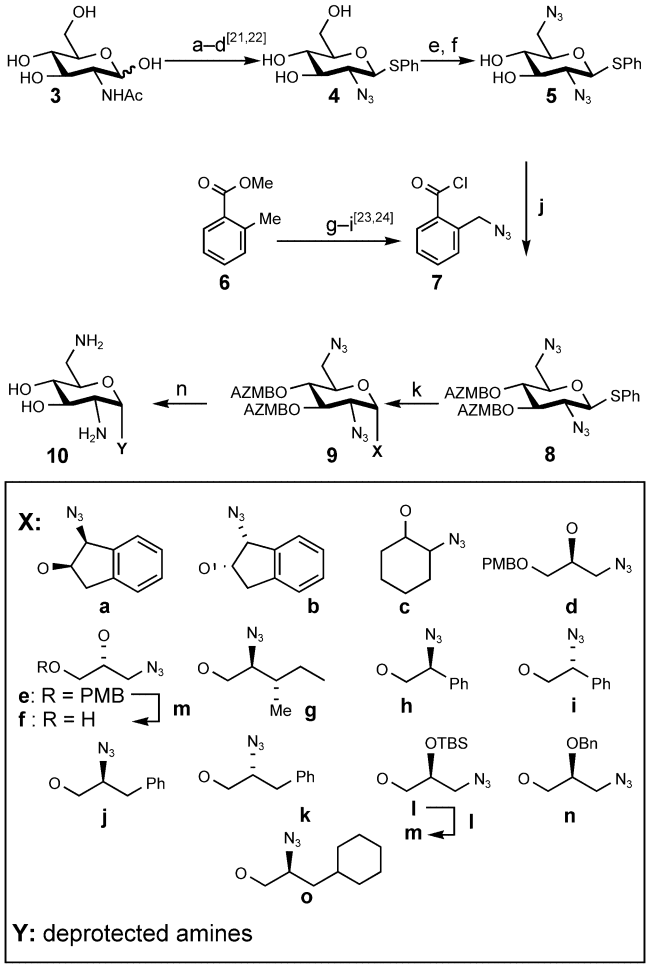

Scheme 1. Reagents and conditions: a) **3** *(1.0 equiv), 4-DMAP (0.05 equiv), Ac_2O (8.0 equiv), Et_3N/CH_2Cl_2 (1:1, 0.25 M), 18 h, 0 → 23 °C, quantitative; b) pentaacetate (1.0 equiv), ZnI_2 (7.0 equiv), PhS-TMS (4.0 equiv), 1,2-dichloroethane (0.2 M), 5 h, 50 °C, 89 %; c) thioglycoside (1.0 equiv), NaOH (1.0 M), 15 h, reflux; d) amine (1.0 equiv), TfN_3[22] (2.0 equiv, 0.5 M in CH_2Cl_2), 4-DMAP (1.0 equiv), MeOH (0.12 M), 16 h, 23 °C, 90 % over two steps; e)* **4** *(1.0 equiv), p-TsCl (1.2 equiv), pyridine (0.17 M), 15 h, 0 → 23 °C, quantitative; f) tosylate (1.0 equiv), NaN_3 (1.2 equiv), DMF (0.26 M), 4 h, 80 °C, 97 %; g) methyl 2-methylbenzoate (1.0 equiv), NBS (1.05 equiv), benzoyl peroxide (0.01 equiv), CCl_4 (0.25 M), 20 h, reflux; then 23 °C, filter, wash with CCl_4, concentrate; then NaN_3 (1.1 equiv), EtOH (0.3 M), 12 h, 84 % for two steps; h) methyl ester (1.0 equiv), LiOH (excess), THF/H_2O (10:1), 60 h, 23 °C, 97 %; i) acid (1.0 equiv), SO_2Cl_2 (3.0 equiv), $CHCl_3$ (0.3 M), 15 h, reflux, concentrate, 97 %; j)* **5** *(1.0 equiv),* **7** *(4.0 equiv), 4-DMAP (4.0 equiv), CH_2Cl_2 (0.2 M), 4 h, 23 °C, 88 %; k)* **8** *(1.0 equiv), XH (**a** – **o**; 1.5 equiv), NIS (2.0 equiv), MS (4 Å), Et_2O/CH_2Cl_2 (4:1, 0.03 M), 2 h, −30 → 0 °C, 61 – 88 %; l)* **l** *(1.0 equiv), TBAF (1.2 equiv), THF (0.1 M), 1 h, 0 → 23 °C, 84 %; m)* **e** *(1.0 equiv), DDQ (1.3 equiv), CH_2Cl_2/H_2O (9:1, 0.2 M), 3 h, 23 °C, 83 %; n)* **9a** – **9o** *(1.0 equiv), Me_3P (8.5 equiv, 1 M in THF), NH_4OH/pyridine (1:7), 4 h, 23 °C, 50 – 92 % isolated yield* **10a** – **10o** *(final structures shown in Table 1). p-TsCl, p-toluenesulfonyl chloride; DMF, N,N-dimethylformamide; NBS, N-bromosuccinimide; NIS, N-iodosuccinimide; TBS, tert-butyldimethylsilyl; TBAF, tetra-n-butylammonium fluoride; THF, tetrahydrofuran; PMB, 4-methoxybenzyl; 4-DMAP, 4-(dimethylamino)pyridine; DDQ, 2,3-dichloro-5,6-dicyano-1,4-benzoquinone; PhS-TMS, phenylthiotrimethylsilane; AZMB, 2-(azidomethyl)benzoyl; MS, molecular sieves; Ph, phenyl; Bn, benzyl; Tf, trifluoromethanesulfonyl.*

The biological activities of the novel aminoglycoside mimetics as inhibitors of bacterial (B_{IVT}) and eukaryotic (E_{IVT}) protein synthesis were evaluated in separate in vitro translation assays that measure the inhibitory effect of compounds on production of luciferase reporter protein in a cell-free system (Table 1).

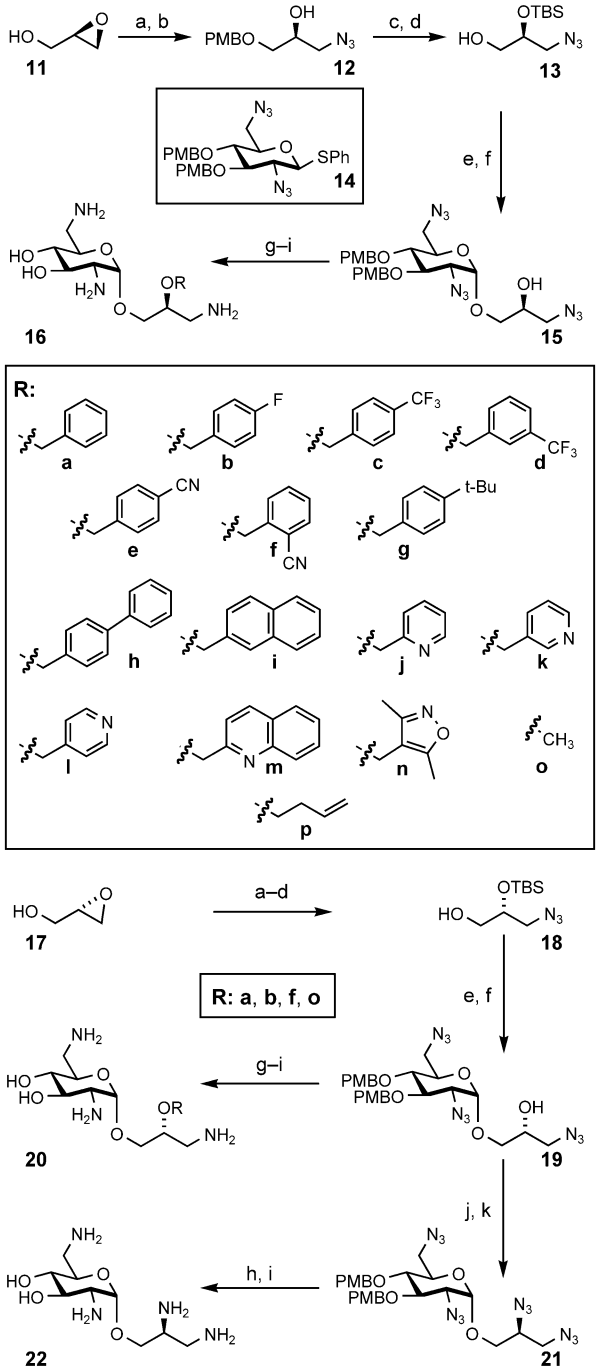

*Scheme 2. Reagents and conditions: a) R-(+)-glycidol (***11***; 1.0 equiv), NaH (1.5 equiv), PMBCl (1.2 equiv), DMF (0.5 M), 4 h, −5 → 23 °C, quantitative; b) epoxide (1.0 equiv), NaN_3 (1.5 equiv), NH_4Cl (2.0 equiv), DMF (0.5 M), 5 h, 90 °C, 93 %; c)* **12** *(1.0 equiv), TBS-OTf (1.5 equiv), 2,6-lutidine (3.0 equiv), CH_2Cl_2 (0.5 M), 1 h, −20 → 23 °C, 93 %; d) PMB-ether (1.0 equiv), CAN (3.0 equiv), MeCN/H_2O (9:1, 0.3 M), 3 h, 23 °C, 86 %; e)* **14** *(1.0 equiv),* **13** *(1.5 equiv), NIS (2.0 equiv), MS (4 Å), Et_2O/CH_2Cl_2 (4:1, 0.03 M), 2 h, −30 → 0 °C; f) silyl-ether (1.0 equiv), TBAF (1.2 equiv), THF (0.1 M), 1 h, 0 → 23 °C, 66 % for two steps; g)* **15** *(1.0 equiv), RCl or RBr (1.5 equiv), NaH (3.0 equiv), TBAI (0.05 equiv), DMF (0.1 M), 68 – 87 %; h) PMB-ethers (1.0 equiv), CAN (4.4 equiv), MeCN/H_2O (9:1, 0.3 M), 3 h, 23 °C, 74 – 91 %; i) Azides (1.0 equiv), Me_3P (8.5 equiv, 1 M in THF), NH_4OH/pyridine (1:7), 4 h, 23 °C, 87 – 95 %* **16a** – **16p** *(final structures shown in Table 1); j)* **19** *(1.0 equiv), MsCl (3.0 equiv), pyridine (0.5 M), 1 h, 0 → 23 °C, quantitative; k) mesylate (1.0 equiv), NaN_3 (10.0 equiv), DMF (0.05 M), 12 h, 50 °C, quantitative; TBAI, tetra-n-butylammonium iodide; CAN, ceric(IV) ammonium nitrate; MsCl, methanesulfonyl chloride; for further abbreviations, see Scheme 1.*

 © 2003 Wiley-VCH Verlag GmbH & Co. KGaA, Weinheim

Table 1. Structure – activity relationships for 6′-aminoglucosamine derivatives and some natural aminoglycosides.

Cpd n°	Structure	$B_{IVT}IC_{50}$[a] $E_{IVT}IC_{50}$ RNA IC_{50} MIC	Cpd n°	Structure	$B_{IVT}IC_{50}$[a] $E_{IVT}IC_{50}$ RNA IC_{50} MIC	Cpd n°	Structure	$B_{IVT}IC_{50}$[a] $E_{IVT}IC_{50}$ RNA IC_{50} MIC	Cpd n°	Structure	$B_{IVT}IC_{50}$[a] $E_{IVT}IC_{50}$ RNA IC_{50} MIC
10h		320 > 250 n.d. n.d.									
10i		600 > 250 n.d. n.d.	**25c**	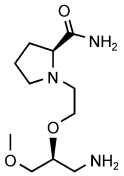	130 1.0 41 > 64/> 64	**16d**	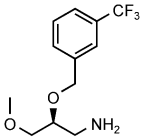	1000 > 250 n.d. n.d.	**16l**	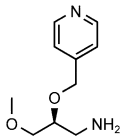	490 > 250 n.d. n.d.
10j	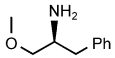	490 > 250 n.d. n.d.	**23**	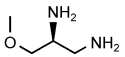	> 1000 n.d. n.d. n.d.						
10k	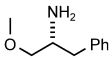	> 1000 > 250 n.d. n.d.	**10o**	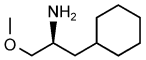	> 1000 > 250 n.d. n.d.	**16e**	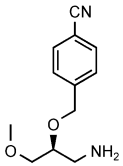	880 > 250 n.d. n.d.	**16m**	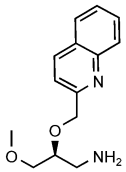	190 36 4.9 > 64/> 64
	Neomycin[c]	0.032 > 250 n.d. 1/0.1		Paromomycin[c]	0.23 > 250 0.59 8/0.5	**16f**	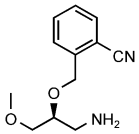	310 > 250 n.d. n.d.	**16n**	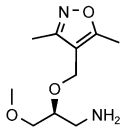	> 1000 > 250 n.d. n.d.
	Neamine[c]	0.37 n.d. n.d. 16/8		Paromamine[c]	3.9 n.d. 14 > 64/64	**20f**	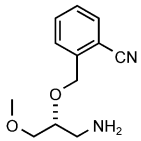	250 > 250 n.d. n.d.			

[a] IC_{50}, concentration required for 50% inhibition. All IC_{50} values are in μM. B_{IVT}: IC_{50} value determined in a coupled bacterial in vitro transcription – translation assay with firefly luciferase reporter, as previously described;[11, 14] IC_{50} values were calculated as the average of six replicate experiments for each compound (± 10%). All compounds tested negative in counter-screens for luciferase and polymerase inhibition. E_{IVT}: IC_{50} value determined in a eukaryotic in vitro translation assay with firefly luciferase reporter; IC_{50} values were calculated as the average of three replicate experiments (± 15%). RNA IC_{50}: IC_{50} value found in a fluorescence-based assay that measures RNA-binding affinity of compounds and their efficacy to flip-out the flexible adenine residues in a decoding site model oligonucleotide (± 10%).[25] MIC: minimum inhibitory concentration [μg mL^{-1}], determined as the average of triplicate measurements in serial dilution against *Escherichia coli* (first value) and *Staphylococcus aureus* (second value). [b] Values reported for a mixture of diastereomers. [c] For structures of the natural aminoglycosides, see Figure 1 a.

© 2003 Wiley-VCH Verlag GmbH & Co. KGaA, Weinheim

Table 1. (Continued)

Cpd n°	Structure	$B_{IVT}IC_{50}$[a] $E_{IVT}IC_{50}$ RNA IC_{50} MIC	Cpd n°	Structure	$B_{IVT}IC_{50}$[a] $E_{IVT}IC_{50}$ RNA IC_{50} MIC	Cpd n°	Structure	$B_{IVT}IC_{50}$[a] $E_{IVT}IC_{50}$ RNA IC_{50} MIC	Cpd n°	Structure	$B_{IVT}IC_{50}$[a] $E_{IVT}IC_{50}$ RNA IC_{50} MIC
10a	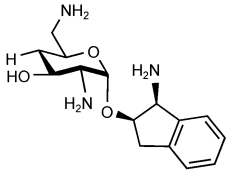	180 40 > 1000 > 64/ > 64	**10m**	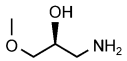	860 31 > 1000 > 64/ > 64	**16a**	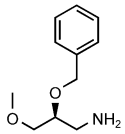	170 > 250 > 1000 > 64/ > 64	**16g**	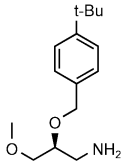	> 1000 > 250 n.d. n.d.
10b	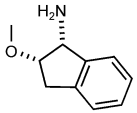	410 33 > 1000 > 64/ > 64	**16o**	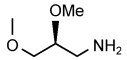	> 1000 n.d. n.d. n.d.						
10c		690 (mix)[b] > 250 n.d. n.d.	**20o**	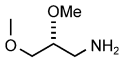	> 1000 n.d. n.d. n.d.	**20a**	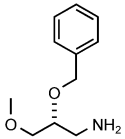	580 > 250 n.d. > 64/ > 64	**16h**	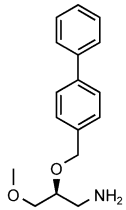	180 22 2.3 > 64/ > 64
10d	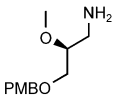	870 > 250 n.d. n.d.	**16p**	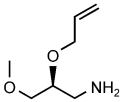	> 1000 88 n.d. n.d.	**16b**	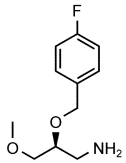	> 1000 > 250 n.d. n.d.	**16i**	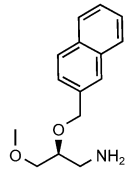	210 49 2.8 > 64/ > 64
10e	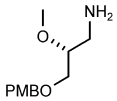	> 1000 > 250 n.d. n.d.									
10f		370 n.d. n.d. > 64/ > 64	**25a**	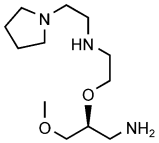	520 > 250 n.d. n.d.	**20b**	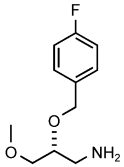	460 > 250 n.d. n.d.	**16j**	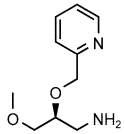	> 1000 > 250 > 1000 > 64/ > 64
10g	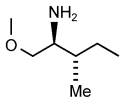	800 > 250 n.d. n.d.	**25b**	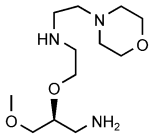	690 > 250 n.d. n.d.	**16c**	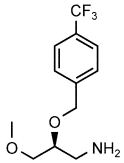	490 > 250 n.d. n.d.	**16k**	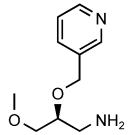	> 1000 > 250 n.d. n.d.

 © 2003 Wiley-VCH Verlag GmbH & Co. KGaA, Weinheim

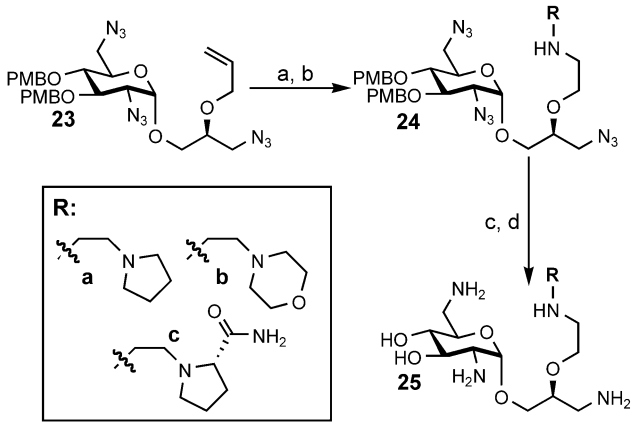

Scheme 3. Reagents and conditions: a) ***23*** *(1.0 equiv), O_3, CH_2Cl_2/MeOH, 10 min, −78 °C; then Me_2S (10.0 equiv), 1 h, −78 → 23 °C; b) aldehyde (1.0 equiv), RNH_2 (4.0 equiv), $NaBH_3CN$ (1.0 equiv), MeOH (0.2 M), AcOH to pH 5.0, 12 h, 23 °C; c)* ***24a–24c*** *(1.0 equiv), Me_3P (8.5 equiv, 1 M in THF), NH_4OH/pyridine (1:7), 4 h, 23 °C; d) PMB-ethers (1.0 equiv), $Pd(OH)_2$ (20 %/C), AcOH, H_2(1 atm), 14 h, 8–19 % overall yield* ***25a–c*** *(final structures shown in Table 1).*

Comparison of inhibition data from the bacterial and eukaryotic assays allows determination of the specificity of the synthesized compounds. Inhibitors of bacterial translation that had an IC_{50} value below 250 μM were tested for binding to the decoding-site target (RNA) by using an RNA fluorescence assay that determines the binding affinity of a ligand based on its ability to flip out the flexible adenine residues A1492 and A1493 in a model oligonucleotide (see Figure 1).[25] The fluorescence assay thus returns a true measure of the potency of a compound for binding specifically to the decoding-site internal loop and inducing a conformational response comparable to that triggered by natural aminoglycoside antibiotics. Compounds that showed an IC_{50} value below 250 μM in the bacterial translation assay were also submitted to growth inhibition tests on *Escherichia coli* and *Staphylococcus aureus* strains to detect potential antibacterial potency (MIC).

The synthesized aminoglycoside mimetics that have biological activity in at least one of the translation assays fall into three classes. The first set, which includes diastereomers of the two indane derivatives **10a** and **10b**, the alcohol **10m**, the allyl ether **16p**, and the proline derivative **25c**, showed no or only weak inhibition in the bacterial translation assay ($IC_{50} \geq 130$ μM) and, accordingly, did not bind to the bacterial decoding-site RNA but were inhibitors of in vitro eukaryotic protein synthesis at concentrations below 100 μM. Interestingly, the proline derivative **25c** was particularly potent against eukaryotic translation ($IC_{50} = 1.0$ μM), but more than 100-fold less active in the bacterial system ($IC_{50} = 130$ μM) and a weak binder of the bacterial decoding-site RNA ($IC_{50} = 41$ μM), which suggests that this compound, and to a lesser extent perhaps also **10m**, **10a**, **10b**, and **16p** selectively target a eukaryotic ribosomal component that is absent in bacteria.

The second set of compounds is comprised of the benzylic ethers with large nonpolar substituents (**16m**, **16i**, **16h**). These compounds bound with low micromolar affinity ($IC_{50} = 2.3$–4.9 μM) to the bacterial decoding-site RNA, and inhibited both bacterial and eukaryotic translation, albeit with higher potency against the eukaryotic system ($IC_{50} = 180$–210 μM versus 22–49 μM). A control experiment in which the eukaryotic decoding-site RNA was used to measure affinity in the fluorescence assay revealed IC_{50} values in the low micromolar range for compounds **16m**, **16i**, and **16h**. Nonspecific intercalation of the flat hydrophobic biphenyl (**16h**), naphtyl (**16i**), and quinolyl (**16m**) substituents may contribute to promiscuous RNA binding of these glucosamine derivatives; they show affinity for both the bacterial and eukaryotic decoding-site RNAs which, however, does not translate into comparably distinct potencies against the targets in the functional translation assay. The considerable differences between the RNA binding affinities of the biphenyl (**16h**) and naphtyl (**16i**) derivatives and that of the parental benzylic ether **16a**, as well as between the affinity of the quinolyl compound **16m** and that of the *o*-picolyl ether **16j** are in line with an intercalative binding mode of **16m**, **16i**, and **16h**.

The benzylic ether **16a** is the only member of a third compound category, which shows selective inhibition of bacterial ($IC_{50} = 170$ μM) but not eukaryotic in vitro translation, yet does not bind to the bacterial decoding-site RNA target. The inhibitory activity of **16a**, and similarly that of the indane derivative **10a**, against the bacterial translation assay in the absence of decoding-site binding suggests that these compounds recognize other targets in the bacterial ribosome. The two- to threefold better potency of **16a** and **10a** compared to their diastereomers **20a** and **10b** demonstrates the stereospecificity of the inhibitory mechanism. Both steric and electronic effects modulate biological activity in the series of substituted benzylic and picolylic ethers, as attested by the range of IC_{50} values determined for these compounds.

Comparison of the biological activities of glucosamine derivatives belonging to Series **1** (Figure 1) and those of the compounds of Series **2** reveals a larger number of representatives in the latter of the classes described above. Molecular modeling studies, which were used to explore the conformational space accessible to the acyclic moieties of the synthesized aminoglycoside mimetics,[20] show that conformations mimicking the paromamine core (Figure 1 d, e) are clearly energetically favorable for the Series **2** compounds, whereas representatives of Series **1** adopted other preferred conformations as well. An exception was the relatively potent derivative **10a**, which was found to occupy a paromamine-like conformation induced by the bulky indane scaffold.

In summary, the structure–activity relationships for the synthetic glucosamine derivatives show that none of the acyclic scaffolds, which were introduced as mimetics of 2-DOS, confer a high potency comparable to that of the natural aminoglycosides. We propose that the increased flexibility of the acyclic 2-DOS mimetics has a detrimental effect on their RNA binding efficacy. In line with the finding of biologically more active aminoglycoside mimetics among cyclic piperidine derivatives,[19] we conclude that the rigidity of the 2-DOS scaffold plays an essential role in the potency of aminoglycoside antibiotics. It has previously been pointed out that natural aminoglycosides provide conformationally constrained molecular scaffolds for the spatially defined presentation of hydrogen-bond-donor

 © 2003 Wiley-VCH Verlag GmbH & Co. KGaA, Weinheim

moieties and positively charged groups, which can participate in an intimate network of interactions with the ribosomal RNA targets.[7, 26] Thus, a simplified mimetic replacing the privileged 2-DOS scaffold of aminoglycosides has yet to be discovered.

Experimental Section

Characteristic analytical data of selected compounds:

Amine 10h: ^{1}H NMR (400 MHz, D_2O): $\delta = 7.50 - 7.38$ (m, 5H), 5.25 (d, $J = 3.6$ Hz, 1H), 4.80 – 4.74 (m, 1H), 4.17 – 4.05 (m, 1H), 3.98 – 3.93 (m, 1H), 3.81 – 3.76 (m, 1H), 3.43 – 3.34 (m, 3H), 3.23 (br d, $J = 13.6$ Hz, 1H), 3.11 – 3.04 (m, 1H) ppm; ^{13}C NMR (100 MHz, D_2O): $\delta = 133.3$, 129.9, 129.6 (2C), 127.3, 127.2, 95.5, 70.7, 69.4, 68.6 (2 C), 54.5, 53.7, 40.0 ppm.

Amine 10j: ^{1}H NMR (400 MHz, D_2O): $\delta = 7.38 - 7.23$ (m, 5H), 5.17 (d, $J = 3.2$ Hz, 1H), 3.92 – 3.82 (m, 3H), 3.78 – 3.70 (m, 2H), 3.42 – 3.36 (m, 2H), 3.31 (dd, $J = 13.6$, 3.2 Hz, 1H), 3.13 (br dd, $J = 13.6$, 8.0 Hz, 1H), 3.04 (dd, $J = 14.8$, 6.8 Hz, 1H), 2.97 (dd, $J = 14.8$, 8.0 Hz, 1H) ppm; ^{13}C NMR (100 MHz, D_2O): $\delta = 135.2$, 129.6, 129.5, 129.4 (2 C), 128.0, 95.6, 70.9, 69.4, 68.7, 67.3, 53.7, 52.4, 40.2, 35.2 ppm.

Quinolinemethyl ether 16m: ^{1}H NMR (400 MHz, D_2O): $\delta = 8.99 - 8.95$ (m, 1H), 8.27 – 8.24 (m, 1H), 8.20 – 8.17 (m, 1H), 8.07 – 8.02 (m, 1H), 7.93 – 7.90 (m, 1H), 7.87 – 7.83 (m, 1H), 5.39 (d, $J = 16.0$ Hz, 1H), 5.24 – 5.18 (m, 2H), 4.27 – 4.25 (m, 1H), 4.02 – 3.98 (m, 1H), 3.90 – 3.85 (m, 1H), 3.81 – 3.72 (m, 2H), 3.40 – 3.32 (m, 5H), 3.15 (dd, $J = 8.5$, 5.2 Hz, 1H) ppm; ^{13}C (100 MHz, D_2O): $\delta = 155.0$, 147.6, 137.5, 135.4, 130.1, 129.4, 128.4, 120.2, 120.0, 95.9, 76.0, 71.1, 69.6, 68.7, 67.9, 66.6, 53.8, 40.7, 40.5 ppm.

Benzyl ether 20a: ^{1}H NMR (400 MHz, D_2O): $\delta = 7.40 - 7.25$ (m, 5H), 4.72 (d, $J = 3.6$ Hz, 1H), 4.62 – 4.56 (m, 2H), 3.77 (dd, $J = 10.8$, 3.6 Hz, 1H), 3.74 – 3.66 (m, 1H), 3.48 – 3.36 (m, 3H), 3.24 – 3.14 (m, 2H), 2.94 (dd, $J = 14.4$, 3.2 Hz, 1H), 2.84 – 2.66 (m, 2H), 2.59 (dd, $J = 10.0$, 3.2 Hz, 1H) ppm; ^{13}C NMR (100 MHz, D_2O): $\delta = 137.6$, 128.9, 128.8, 128.7, 128.6, 128.5, 99.5, 78.6, 74.3, 72.3, 72.1, 71.8, 67.6, 55.3, 41.7, 41.6 ppm.

Prolinamide 25c: ^{1}H NMR (400 MHz, D_2O): $\delta = 5.13$ (d, $J = 3.6$ Hz, 1H), 4.32 (dd, $J = 5.6$, 10.0 Hz, 1H), 4.07 – 4.01 (m, 1H), 3.89 – 3.73 (m, 6H), 3.64 (br dd, $J = 3.6$, 11.2 Hz, 3H), 3.54 – 3.44 (m, 2H), 3.42 – 3.30 (m, 4H), 3.29 – 3.02 (m, 1H), 2.59 – 2.46 (m, 1H), 2.16 – 2.04 (m, 2H), 1.96 – 1.84 (m, 1H) ppm; ^{13}C NMR (100 MHz, D_2O): $\delta = 170.7$, 94.9, 74.3, 70.0, 68.4, 67.6, 66.6, 66.1, 64.1, 56.3, 54.6, 52.5, 39.6, 39.3, 29.5, 22.0 ppm.

We thank B. Aust for determining MIC values and Dr. K. Steffy for help with the eukaryotic in vitro translation assay. This work was supported in part by a National Institutes of Health grant to T.H.

[1] E. F. Gale, E. Cundliffe, P. E. Renolds, M. H. Richmond, M. J. Waring, *The Molecular Basis of Antibiotic Action* John Wiley & Sons, London, **1981**.

[2] a) D. Moazed, H. F. Noller, *Nature* **1987**, *327*, 389 – 394; b) P. Purohit, S. Stern, *Nature* **1994**, *370*, 659 – 662; c) C.-H. Wong, M. Hendrix, E. S. Priestley, W. A. Greenberg, *Chem. Biol.* **1998**, *5*, 397 – 406.

[3] a) V. Ramakrishnan, *Cell* **2002**, *108*, 557 – 572; b) D. Fourmy, S. Yoshizawa, J. D. Puglisi, *J. Mol. Biol.* **1998**, *277*, 333 – 345.

[4] J. M. Ogle, D. E. Brodersen, W. M. Clemons, M. J. Tarry, A. P. Carter, V. Ramakrishnan, *Science* **2001**, *292*, 897 – 902.

[5] a) L. P. Kotra, J. Haddad, S. Mobashery, *Antimicrob. Agents Chemother.* **2000**, *44*, 3249 – 3256; b) G. D. Wright, A. M. Berghuis, S. Mobashery in *Resolving the Antibiotic Paradox: Progress in Understanding Drug Resistance and Development of New Antibiotics* (Eds.: B. P Rosen, S. Mobashery), Plenum, New York, **1998**, pp. 27 – 69.

[6] R. Schroeder, C. Waldsich, H. Wank, *EMBO J.* **2000**, *19*, 1 – 9.

[7] Y. Tor, T. Hermann, E. Westhof, *Chem. Biol.* **1998**, *5*, R277 – R283.

[8] a) T. Hermann, E. Westhof, *Biopolymers* **1999**, *48*, 155 – 165; b) T. Hermann, *Angew. Chem.* **2000**, *112*, 1962 – 1979; *Angew. Chem. Int. Ed.* **2000**, *39*, 1890 – 1904.

[9] a) K. Michael, Y. Tor, *Chem. Eur. J.* **1998**, *4*, 2091 – 2098; b) S. J. Suchek, Y.-K. Shue, *Curr. Opin. Drug Discovery Dev.* **2001**, *4*, 462 – 470; c) T. Hermann, *Biochimie* **2002**, *84*, 865 – 875.

[10] Y. Ding, S. A. Hoftstadler, E. E. Swayze, R. H. Griffey, *Org. Lett.* **2001**, *3*, 1621 – 1623.

[11] D. Vourloumis, M. Takahashi, G. C. Winters, K. B. Simonsen, B. K. Ayida, S. Barluenga, S. Qamar, S. Shandrick, Q. Zhao, T. Hermann, *Bioorg. Med. Chem. Lett.* **2002**, *12*, 3367 – 3372.

[12] a) P. Alper, M. Hendrix, P. Sears, C.-H. Wong, *J. Am. Chem. Soc.* **1998**, *120*, 1965 – 1978; b) W. A. Greenberg, E. S. Priestley, P. S. Sears, P. B. Alper, C. Rosenbohm, M. Hendrix, S.-C. Hung, C.-H. Wong, *J. Am. Chem. Soc.* **1999**, *121*, 6527 – 6541; c) C. L. Nunns, L. A. Spence, M. J. Slater, D. J. Berrisford, *Tetrahedron Lett.* **1999**, *40*, 9341 – 9345; d) J. Haddad, L. P. Kotra, B. Llano-Sotelo, C. Kim, E. F. Azucena, M. Liu, S. B. Vakulenko, C. S. Chow, S. Mobashery, *J. Am. Chem. Soc.* **2002**, *124*, 3229 – 3237.

[13] S. Hanessian, M. Tremblay, A. Kornienko, N. Moitessier, *Tetrahedron* **2001**, *57*, 3255 – 3265.

[14] K. B. Simonsen, B. K. Ayida, D. Vourloumis, M. Takahashi, G. C. Winters, S. Barluenga, S. Qamar, S. Shandrick, Q. Zhao, T. Hermann, *ChemBioChem* **2002**, *3*, 1223 – 1228.

[15] C.-H. Wong, M. Hendrix, D. D. Manning, C. Rosenbohm, W. A. Greenberg *J. Am. Chem. Soc.* **1998**, *120*, 8319 – 8327.

[16] a) Q. Vicens, E. Westhof, *Structure* **2001**, *9*, 647 – 658; b) Q. Vicens, E. Westhof, *Chem. Biol.* **2002**, *9*, 747 – 755.

[17] D. Fourmy, M. I. Recht, S. C. Blanchard, J. D. Puglisi, *Science* **1996**, *274*, 1367 – 1371.

[18] A. P. Carter, W. M. Clemons, D. E. Brodersen, R. J. Morgan-Warren, B. T. Wimberly, V. Ramakrishnan, *Nature* **2000**, *407*, 340 – 348.

[19] See the following communication: K. B. Simonsen, B. K. Ayida, D. Vourloumis, G. C. Winters, M. Takahashi, S. Shandrick, Q. Zhao, T. Hermann, *ChemBioChem* **2003**, *4*, 886 – 890.

[20] Molecular modeling was performed by using published atom coordinates of the 30S ribosomal subunit – aminoglycoside complexes[4,18] and high-resolution crystal structures of synthetic RNA constructs containing the bacterial decoding-site internal loop (Q. Zhao, T. Hermann, unpublished results). Preferred conformations of the novel aminoglycoside mimetics **1** and **2** were explored by molecular dynamics simulations and energy minimization by using the Insight/Discover software (Accelrys, San Diego) and following established protocols.[26]

[21] T. Buskas, P. J. Garegg, P. Konradsson, J.-L. Maloisel, *Tetrahedron: Asymmetry* **1994**, *5*, 2187 – 2194.

[22] a) C. J. Cavender, V. J. Shiner, *J. Org. Chem.* **1972**, *37*, 3567 – 3569; b) P. B. Alper, S.-C. Hung, C.-H. Wong, *Tetrahedron Lett.* **1996**, *37*, 6029 – 6032.

[23] T. Wada, A. Ohkubo, A. Mochizuki, M. Sekine, *Tetrahedron Lett.* **2001**, *42*, 1069 – 1072.

[24] K. R. Love, R. B. Andrade, P. H. Seeberger, *J. Org. Chem.* **2001**, *66*, 8165 – 8176.

[25] S. Shandrick, Q. Zhao, Q. Han, T. Hermann, unpublished work.

[26] a) T. Hermann, E. Westhof, *J. Mol. Biol.* **1998**, *276*, 903 – 912; b) T. Hermann, E. Westhof, *J. Med. Chem.* **1999**, *42*, 1250 – 1261.

Received: June 12, 2003 [Z688]

 © 2003 Wiley-VCH Verlag GmbH & Co. KGaA, Weinheim